Layered composite membranes based on porous PVDF coated with a thin, dense PBI layer for Vanadium Redox Flow Batteries

Wonmi Lee,[1#] Mina Jung,[1,2#] Dmytro Serhiichuk,[2,3,4] Chanho Noh,[1] Gaurav Gupta,[5] Corinna Harms,[5] Yongchai Kwon,*[1] Dirk Henkensmeier**[2,3,6]

1 Graduate School of Energy and Environment, Seoul National University of Science and Technology, Nowon-gu, Seoul 139-743, Korea
2 Center for Hydrogen and Fuel Cell Research, KIST, Seoul 02792, Korea
3 Division of Energy & Environment Technology, KIST School, University of Science and Technology, Seoul 02792, Korea
4 NTUU Igor Sykorsky Kyiv Polytechnic Institute, Kyiv 03056, Ukraine
5 Fuel Cells, DLR-Institut für Vernetzte Energiesysteme e.V., 26129 Oldenburg, Germany
6 Green School, Korea University, Anam-ro 145, Seongbuk-gu, Seoul 02841, Korea

#Both contributed equally

* kwony@seoultech.ac.kr

** henkensmeier@kist.re.kr

Abstract

A commercial porous polyvinylidene fluoride membrane (pore size 0.65 µm, nominally 125 µm thick) is spray coated with 1.2 - 4 µm thick layers of polybenzimidazole. The area resistance of the porous support is 36.4 mΩ cm^2 in 2M sulfuric acid, in comparison to 540 mΩ cm^2 for a 27 µm thick acid doped polybenzimidazole membrane, and 124 mΩ cm^2 for PVDF-P20 (4 µm thick blocking layer). Addition of vanadium ions to the supporting electrolyte increases the resistance, but less than for Nafion. The expected reason is a change in the osmotic pressure when the ionic strength of the electrolyte is increased, reducing the water contents in the membrane. The orientation of the composite membranes has a strong impact. Lower permeability values are found when the blocking layer is oriented towards the vanadium-lean side in ex-situ measurements. Cells with the blocking layer on the positive side have significantly lower capacity fade, also much lower than cells using Nafion 212. The coulombic efficiency of cells with PVDF-PBI membranes (98.4%)

is higher than that of cells using Nafion 212 (93.6%), whereas the voltage efficiency is just slightly lower, resulting in energy efficiencies of 85.1 and 83.3%, respectively, at 80 mA/cm^2.

Keywords: porous PVDF; polybenzimidazole blocking layer; composite membranes; Vanadium Redox Flow Batteries

1. Introduction

Redox flow batteries are electrochemical energy storage devices which consist of two half cells, separated by a membrane.[1-4] In charged vanadium redox flow batteries (VRFB), one half cell is filled with a solution containing V^{2+} ions, while the other half cell contains a solution with V^{5+} ions.[5-7] During discharge, V^{2+} is oxidized to V^{3+}, and V^{5+} is reduced to V^{4+}. The opposite reactions take place when the cell is charged. Therefore, the output power is determined by the active cell area, while the capacity (stored energy) is based on the size of the electrolyte storage tanks. These features make flow batteries very attractive as energy storage solutions in combination with fluctuating sources of renewable energy. For example, Fraunhofer ICT combined a 2 MW wind turbine with flow batteries connected to 45,000 liter storage tanks for the electrolytes, producing a battery capacity of 20 MWh.[8]

Since the electrolyte solutions are typically aqueous 1.5-3 M sulfuric acid solutions of vanadium ions, the membranes should show a high chemical resistance against acids and highly oxidative V^{5+} ions.[9] In addition, they should show a high conductivity for charge carriers like protons or sulfate but should block permeation of redox active species.[10] While perfluorinated Nafion membranes show an excellent stability and low resistance, they are cation exchange membranes and thus allow permeation of vanadium ions, resulting in a relative low coulomb efficiency (CE). This problem is typically addressed by increasing the thickness of the membranes, on the cost of resistance. Alternative materials which conduct selectively anions would help, but they are most commonly made from electron rich hydrocarbons, which are easily attacked by V^{5+}.[11]

An excellent solution seems to be the use of polybenzimidazole (PBI) based membranes.[12-17] In contact with sulfuric acid, the imidazole groups of PBI are protonated, and absorption of additional sulfuric acid molecules by hydrogen bond interactions leads to proton and sulfate conducting membranes. Apparently, the positive charge on the polymer backbone retards oxidative degradation of the polymer. Furthermore, similar to an anion exchange membrane, the positive charge on the polymer backbones (Donnan exclusion) in combination with the narrow space between the polymer channels (size exclusion for large vanadium ions) leads to a very low

vanadium permeation though PBI membranes. In fact, during an ex-situ test, no permeated V^{4+} ions could be observed by UV-VIS spectroscopy even after 10 days. Nevertheless, the CE of a PBI based cell is close to but lower than 100%. There are two possible reasons for this: a) migration in the electric field provides some vanadium ions with the energy needed to enter the membrane; b) CE is reduced by side reactions (hydrogen evolution).[14] Both mechanisms should correlate with the applied charging voltage, and indeed a slightly higher CE was observed for thinner membranes (lower resistance and thus lower average charging voltage), in contrast to Nafion based cells, which show lower CE (but higher VE) when the membrane thickness is reduced.

In the past, there have been some reports on bilayer membranes, in which a thin blocking layer provides high selectivity while the bulk of the membrane shows a high conductivity. Examples are porous supports coated with Nafion[18] or PIM-1[19], a non-conductive polymer with narrow voids between kinked polymer chains which get filled with the electrolyte and hinder passage of vanadium ions by size exclusion. In other work, Nafion was coated with layers of positively charged polymers, like protonated poly(*N*,*N*-dimethylaminoethyl methacrylate)[20], poly(ethyleneimine)[21], or electrolyte doped PBI[22]. Kim et al. coated sulfonated poly(arylene ether)[23] and an imidazole functionalised PBI membrane with Nafion[24], to protect the bulk membrane material against attack from VO_2^+.

In our previous work, we hypothesised that application of a thin PBI blocking layer to a porous Nafion membrane should lead to a membrane with both high VE and CE.[25] This specific work was challenged by a) the different swelling behavior of PBI and Nafion, which may have induced cracks or pinholes, b) a high resistance of the layer between Nafion and PBI which was needed to promote adhesion, and c) the slow kinetics for filling the closed pores of porous Nafion with electrolyte.

In this work, we apply a thin PBI layer on a porous poly(vinylidene difluoride) (PVDF) support. The commercial support has an open pore structure, which should facilitate filling with electrolyte, and no adhesive layer is needed, because PVDF is only partially fluorinated. Furthermore, PVDF does not show significant swelling in water, which should enhance the life time of the laminated structure. A very similar approach is currently developed by Oldenburg and Gubler, who spray coat porous Treopore PDA30 with a thin PBI blocking layer.[26] In contrast to previously published work, we also look at the effect of the blocking layer's orientation on efficiencies and capacity loss, and qualitatively explain the mechanisms leading to the observed differences.

2. Experimental Part

2.1 Materials

PBI fibers and 14 μm thick (ca. 26 μm in the swollen state) PBI membranes were purchased from Danish Power Systems. The porous PVDF membrane was purchased from Merck Millipore (Durapore Membrane Filter DVPP00010, as specified by Merck Millipore: hydrophilic PVDF, pore size 0.65 μm, 125 μm thickness, 70% porosity). Ethanol was purchased from Sigma Aldrich. Potassium hydroxide flakes were obtained from Daejung Chemical.

2.2 Preparation of the PVDF membranes with a thin PBI layer

PBI fibers were dissolved in 2.5% KOH/ethanol solution to obtain a 1wt% solution. A PVDF membrane of 6cm x 6cm size was placed inside of a plastic frame which has 4cm x 4cm size hole and the edge of the plastic frame was fixed with metal clamps. PBI solution was added in a spray gun (GP-2 produced by Richpen, Japan), and then was horizontally and vertically sprayed on the more dense side of the dry membrane. For each layer, the membrane was coated once in all directions. After each spraying time, sprayed layers were dried by nitrogen gas from the spray gun. Membranes were dried in the vacuum oven at 60 °C for 2 hours to evaporate ethanol. Dried membranes were immersed in DI water overnight to remove KOH from the PBI layer, and again dried for 24 hours at 60 °C in the vacuum. The PBI coated PVDF membranes are denominated as PVDF-Px, where x indicates the number of applied layers (6, 12 or 20).

2.3 Membrane characterisation

Vanadium ion permeability was measured in a cell which consisted of two compartments, separated by the membrane sample. One compartment was filled with 1.5 M $VOSO_4$ in 2 M H_2SO_4 (enriched side) and the other was filled with 1.5 M $MgSO_4$ in 2 M H_2SO_4 (deficient side). At regular intervals samples were drawn from the deficient side into a cuvette, which was placed into an Agilent Technologies Cary 100 UV/Vis spectrometer to detect VO^{2+} ions. The intensity of the peak at 765 nm was used for analysis of the VO^{2+} concentration. The permeability coefficient P [$m^2\ s^{-1}$] was calculated according to

$$P\ [m^2\ s^{-1}] = \frac{1}{C_V}\left(\frac{\Delta C_{M(t)}}{\Delta t}\right)\left(\frac{LV_M}{A}\right).$$

C_V is the vanadium concentration in the $VOSO_4$ solution, the second term is the slope of the quasi-linear trend when the vanadium ion concentration in the $MgSO_4$ solution is plotted against the time,

L is the membrane thickness, V_M is the volume of the $MgSO_4$ solution, A is the effective membrane area.[27]

SEM graphs were measured with an Inspect F50 SEM (FEI) instrument. Samples were prepared by freeze-breaking membranes in liquid nitrogen and sputtering the samples with platinum.

Conductivity was measured in a through-plane cell, which consists of two electrolyte-filled compartments separated by the membrane. During impedance measurements, a small alternating current is applied over the membrane, using gold-coated disc electrodes. Membrane resistance was obtained by subtracting the resistance of the cell without membrane from the resistance of the cell with membrane. For calculation of the conductivity, the thickness of the electrolyte swollen membranes was used.

2.4 VRFB cell tests

A cell kit with an active area of 4 cm^2 was used. Carbon felt (Toyobo XF30A, thickness 3.5 mm) was used for the electrodes, without applying any pre-treatment. The composite membranes were assembled so that the PBI layer was directed to the positive electrode. 1.5 M $VOSO_4$ dissolved in 2 M H_2SO_4 was used as electrolyte in both reservoirs, 15 ml at the negative electrode, 17 ml at the positive electrode. The pump rate was 22 ml min^{-1}. During the activation process, VO^{2+} was converted into VO_2^+ in the positive side by oxidation, while VO^{2+} was reduced to V^{3+} in the negative side. After the activation process, VO_2^+ solution was disposed and the positive reservoir was filled again with VO^{2+} solution. Then, at room temperature, the cell was repeatedly charged up to a voltage of 1.7 V and discharged down to a voltage of 0.8 V at a fixed current density of 80 mA cm^{-2} (ca. 2.5 hours per cycle).

3. Results and Discussion

3.1 Membrane fabrication

Membranes were prepared by spray coating a commercially available PVDF based filtration membrane. SEM analysis of the commercial membrane showed that the side in contact with the cover film has a more open pore structure (**Figure 1a,b**). To achieve a dense, defect free layer, the PBI coating was applied on the denser side. While already a few coating layers give a visually homogenously coated impression (**Supporting Information, Figure S1),** SEM analysis of the membrane surface revealed several potential defects when only 6 layers were applied (**Figure 1c**).

A membrane coated by 20 PBI layers seems to be defect free (**Figure 1d**), and analysis of the cross-sectional area showed that the PBI layer has an average thickness of 3.5 µm **(Figure 1e,f**). This correlated well with the calculated thickness, based on the weight gain during spraying. After washing the membrane with water to remove KOH, the weight gain was about 0.5 mg/cm^2. Assuming a density of 1.3 g cm^{-3} for PBI[28], this relates to a thickness of 3.8 µm. A slightly higher value by gravimetric method can be expected, because some material must have entered the pores. For 6 and 12 applied PBI layers, the thickness was determined as 1.2 and 2.1 µm, respectively. In conclusion, the spraying process allowed to exactly control the thickness of the PBI coating layer, and each applied PBI layer increased the thickness by 0.2 µm.

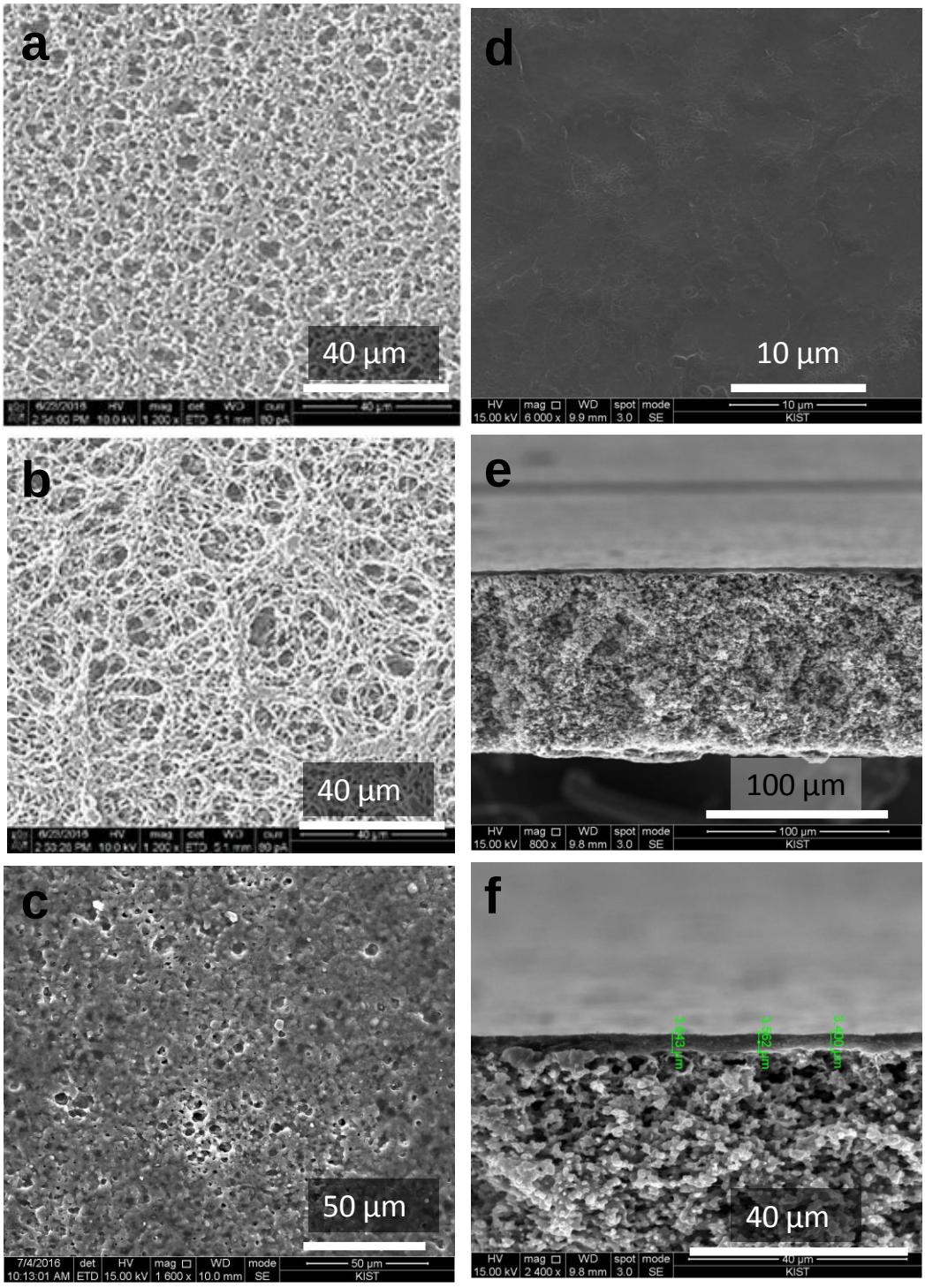

Figure 1: SEM images of the porous PVDF membrane: the more dense side (a), the more open side (b), the PBI coated surface of a PVDF-P6 membrane (c) and for a PVDF-P20 membrane the PBI coated surface (d), and cross-sectional area (e, f).

While 14 µm thick PBI is a strong material with a tensile strength of 123 ± 8.9 MPa, the tensile strength of the porous PVDF support was determined as 6.2 ± 0.3 MPa. A PVDF support coated with 2 µm PBI showed a tensile strength of 7.4 ± 0.8 MPa.

3.2 Membrane Permeability

The permeability of the membranes for VO^{2+} ions was analysed by separating a sulfuric acid filled chamber and a chamber filled with vanadium salt solution in sulfuric acid with a membrane, and monitoring the increasing concentration of VO^{2+} ions in the vanadium deficient chamber by UV/VIS spectrometry. As shown in **Figure 2a**, the vanadium ion concentration increased most rapidly when the cells were separated by 25 µm thick (dry state) Nafion 211. Nafion 212, which is 50 µm thick in the dry state, already showed a much lower permeability. Even lower permeabilities were observed for PVDF-P6, PVDF-P12 and PVDF-P20 membranes. Since PBI has a remarkably low vanadium ion permeability, we assume that the observed flux for PVDF-P6 is strongly influenced by defects in the PBI coating layer. The number of such defects is expected to decrease with each additional coating layer. The permeability coefficients were 4.9, 1.8, 1.3 and 0.5 x 10^{-11} m^2 s^{-1} for N211, N212, PVDF-P6 and PVDF-P12, respectively. These values seem to be a little high. For example, others reported 1.3 x10^{-12} m^2 s^{-1} [29] and 3.2 x 10^{-12} m^2 s^{-1}[30] for N212. On the other hand, these values are lower than values reported for other layered membranes, which were in the range of 10^{-9}-10^{-11}[18, 21, 23, 24], and permeability also depends on the pretreatment of the membranes.[31] For PVDF-P20, no permeability could be calculated during the first 4 hours, because the measured concentration did not increase enough. In a second test, the measurement time was prolonged to 48 hours, and the permeability constants were determined to be 1.1 x 10^{-12} and 5.8 x 10^{-13} m^2 s^{-1} when the PBI layer was directed to the magnesium and the vanadium side, respectively. The effect of the direction of the PBI layer on the observed permeability can be explained by Fick's 1st law. When PBI is directed to the vanadium lean side, permeated vanadium ions are rapidly transported away by the stirred magnesium solution, resulting in a constantly high concentration gradient over the PBI layer (**Figure 2 c)**. When the PBI layer is directed to the vanadium rich side, permeated vanadium ions remain close to the PBI layer, because there is no forced convection in the pores. This leads to a strongly reduced concentration gradient over the PBI layer (**Figure 2 d)**.

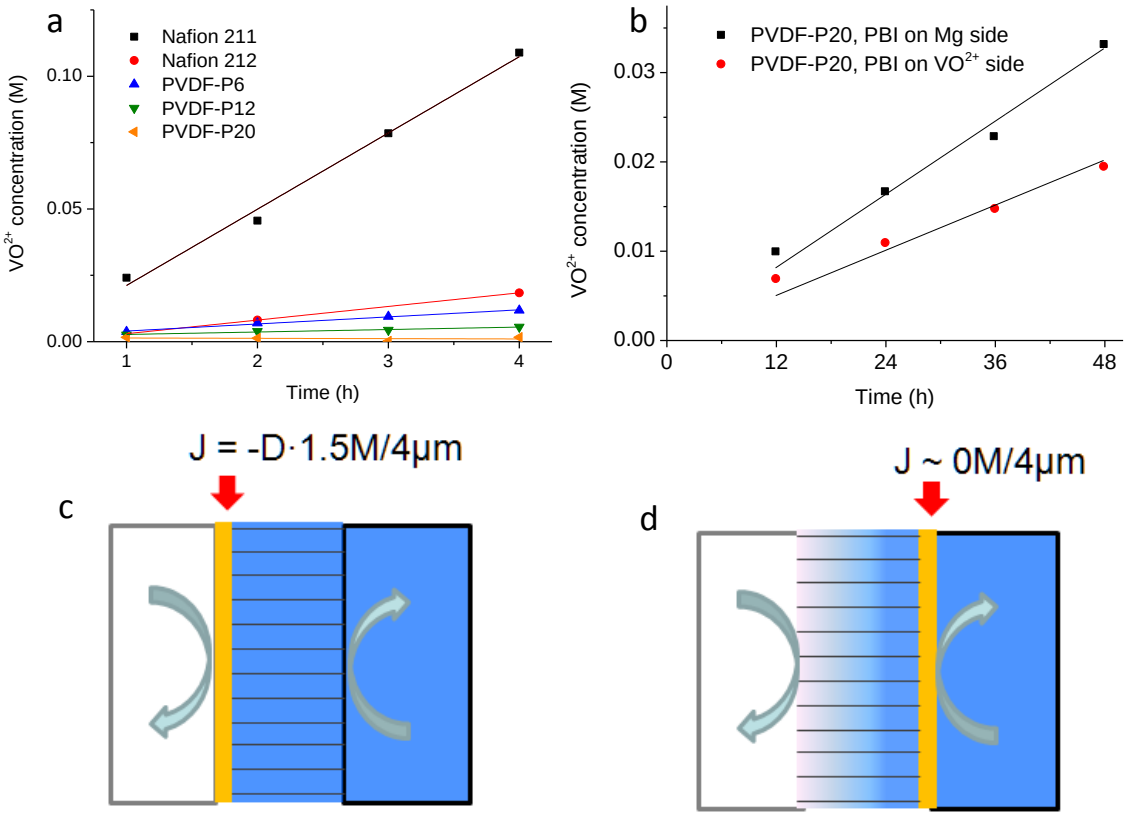

Figure 2: Vanadium permeability a) over 4 hours for Nafion and PBI coated P-PVDF membranes; the PBI layer was directed to the vanadium solution. b) for 48 hours for PVDF-P20, measured in a flow battery set-up with 32 ml solution on each side. c), d) explanation why permeability is lower when a 4 µm thick PBI layer is directed towards the vanadium rich side.

3.3 Membrane Resistance

The voltage efficiency (VE) of flow batteries strongly depends on the membrane resistance, expressed as the area specific resistance (ASR). While the membrane conductivity is a material property, the ASR depends on the membrane thickness. As shown in **Figure 3**, the ion conductivity of *meta*-PBI membranes in 2M sulfuric acid is rather low, around 5 mS cm^{-1}. Shaped into a 27 µm thick membrane, this leads to an ASR of 540 mΩ cm^2, which is between literature values of Nafion 112 and Nafion 117[32] (however, those values were measured in 0.5M sulfuric acid (SA), and increasing the acid concentration reduces the water content and thus the ion conductivity of Nafion).

Within the series of PBI coated porous PVDF membranes, the perceived ion conductivity decreases with increasing thickness of the PBI layer, and the ASR increases. However, the ASR of PVDF-P20, which showed a high repulsion of vanadium ions in the permeability test, is just 124 mΩ cm^2, much lower than the ASR of 14 µm thick PBI (540 mΩ cm^2, wet thickness 27 µm) and only slightly higher than the ASR of Nafion 212 (85 mΩ cm^2). Obviously, the ASR of thicker Nafion membranes (e.g. Nafion 115 is nominally 2.5 times thicker than Nafion 212) would be even higher. The conductivity of Nafion 212 was measured as 68 mS cm^{-1}.

The contributions from the porous, electrolyte filled PVDF membrane and the PBI blocking layer can be obtained by plotting the ASR values against the number of applied PBI layers. The y-axis intercept of the highly linear trend indicates that the ASR of the PVDF membrane is 36.4 mΩ cm^2. Based on this, the ASR of the applied PBI layers of 1.2, 2.4 and 4 µm thickness can be calculated to be 26.7, 51.7 and 87.7 mΩ cm^2, respectively, referring to a conductivity of 4.6 mS/cm, very similar to the 4.8-5.0 mS cm^{-1} obtained for homogeneous PBI membranes in our lab. In conclusion, the ASR of the porous support membrane is far smaller than that of Nafion membranes, and a high Voltage efficiency (VE) can be expected from PBI coated PVDF membranes.

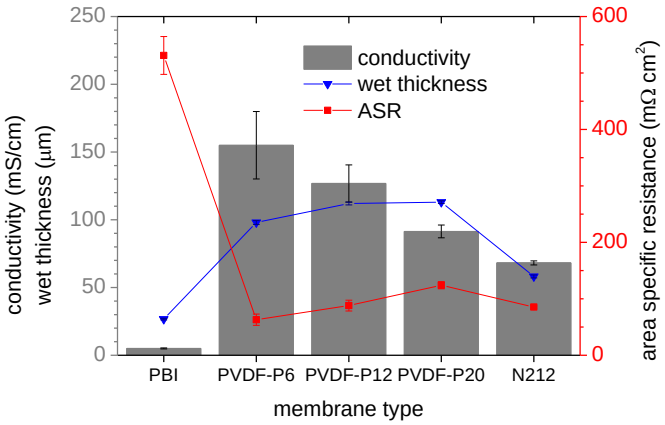

Figure 3: Conductivity and area specific resistance (ASR) in 2M SA at room temperature. The wet thickness of PBI was 26.8 µm.

One effect which should further increase the VE of PBI based systems in comparison to Nafion based systems is the effect of vanadium ions on the membrane resistance. For Nafion 117 in 5M sulfuric acid, it was reported that addition of 1M and 1.75M VO^{2+} decreased the conductivity by about 32% and 53%, respectively, because protons within the membrane were exchanged into less conductive vanadium ions.[33] In our work, the conductivity of Nafion 117 decreased by 69% from 56.2 mS/cm to 17.4 mS/cm when 1.8M VO^{2+} were added to a 2M sulfuric acid solution

(**Figure 4**). This decreasing effect should be smaller for PBI membranes, which repel vanadium ions. Nevertheless, the conductivity of PBI decreased significantly from 3.1 mS/cm to 1.5 mS/cm (52% decrease), when 1.8M VO^{2+} was added. The probable reason for this decrease is the increased osmotic pressure difference over membrane and solution, which reduces the water contents of the membrane.[34, 35] In conclusion, since addition of vanadium ions decreases the resistance of PBI less strongly than that of Nafion, the VE of PBI coated PVDF membranes could be closer to that of Nafion than expected based on the conductivity in sulfuric acid.

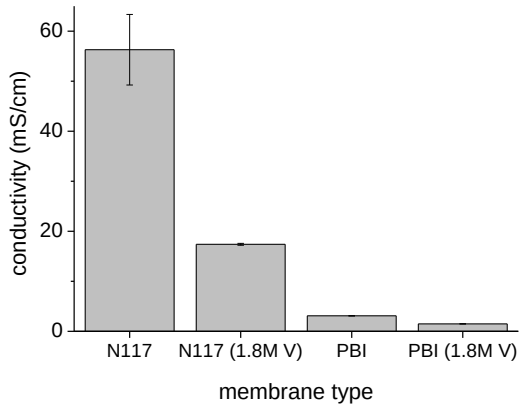

Figure 4: Effect of the addition of 1.8M VO_2^+ to 2M sulfuric acid on the conductivity of Nafion 117 and PBI; the temperature was controlled to 20 °C.

3.4 Performance in the flow battery

The performance in the full cell was tested for Nafion 212 and PVDF-P20. Because the permeability test showed a strong dependence on the orientation of the PBI layer, PVDF-P20 was tested with the PBI layer directed towards the positive and towards the negative electrolyte (**Figure 5a,b,c**). As expected from the permeability test, the CE was significantly higher for the PBI coated PVDF membranes than for Nafion 212. While the VRFB using Nafion 212 showed a CE of 93.6% after 20 charge/discharge cycles at 80 mA/cm^2, the VRFB using PVDF-P20 (PBI on the negative side) reached 97.7% and the cell with PVDF-P20 (PBI on the positive side) reached a slightly higher CE of 98.4%.

Considering the VE, the approach to use a thin PBI membrane supported by PVDF proved to be very successful. While the VE of VRFBs using 15 and 35 µm thick PBI membranes was just 78 and 68%, respectively,[14] the VE of VRFBs using PVDF-P20 was very similar for both tested

orientations, and in the range of 85.3-86.5%, close to the 88.1% achieved by a VRFB using a Nafion 212 membrane (86.3% in [14]).

Consequentially, the energy efficiency (EE) of the cells equipped with Nafion 212, PVDF-P20 (positive side) and PVDF-P20 (negative side) was 82.5%, 85.1% and 83.3%, respectively. Therefore, in terms of efficiency, the coated PVDF membranes seem to perform best when the PBI layer is directed towards the positive electrolyte. In comparison to literature data, the EE of the VRFB using PVDF-P20 (positive side) is high.[36] The EE of a porous ab-PBI membrane was reported to be 87% at 40 mA cm^{-2}, but the practically linear decrease of the EE in that work allows to predict an EE of just 79% at 80 mA cm^{-2}.[37] The apparently highest EE reported so far at 80 mA cm^{-2} is 90%, and was achieved by Li et al. with a VRFB using a 34 µm thick porous O-PBI membrane.[15] The decreasing trend which was observed for VE and EE is probably not related to the membranes, but to changes in the surface chemistry of the electrodes, where loss of hydrophilic groups increases kinetic and mass transport losses.[38]

When comparing PVDF supported PBI and free standing PBI films, PVDF-PBI membranes show a slightly lower voltage and energy efficiency (**Figure 6**), because of the additional ASR contribution of the porous support and because some PBI enters the pores during spray coating. This increases the average thickness and decreases the average area of the PBI layer, and thus increase the ASR of PVDF-P membranes. However, thin, self-supporting PBI membranes may easily get damaged during handling, and in contact with carbon felts, carbon fibers may easily poke through thin membranes, leading to short circuits. Therefore, PVDF-PBI membranes are a good way to balance performance and stability.

Another important measure is the capacity retention during cycling. As expected from the high CE and low ex-situ crossover values, the cell with a PVDF-PBI20 membrane in which the PBI layer was directed to the positive electrolyte showed the most stable charge capacity (the capacity that was charged in one cycle) over the tested 20 cycles (**Figure 7a**). As often observed for Nafion membranes, the charge capacity decreased rapidly over the first cycles, after which the further decrease followed a rather linear trend of 82 $mAhL^{-1}$/cycle, which is slightly higher than the charge capacity loss rate of the cell with PVDF-P20 (positive side), which was just 73 $mAhL^{-1}$/cycle. In strong contrast to this, PVDF-P20 (negative side) showed a catastrophic loss rate of 403 $mAhL^{-1}$/cycle. A repeat experiment with 3 fresh membranes confirmed this result (**Figure 7b**).

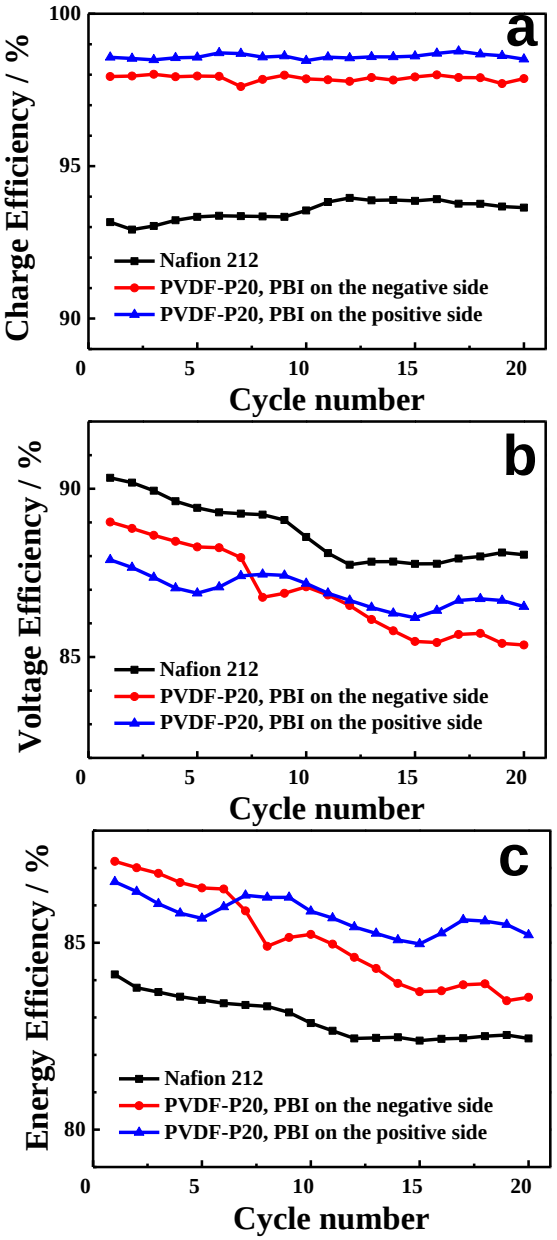

Figure 5: VRFB full cell test results for Nafion 212 and PBI coated P-PVDF, current density 80 mA/cm^2. (a) Charge efficiency (b) Voltage efficiency (c) Energy efficiency; the first 3 cycles (startup phase) are not shown.

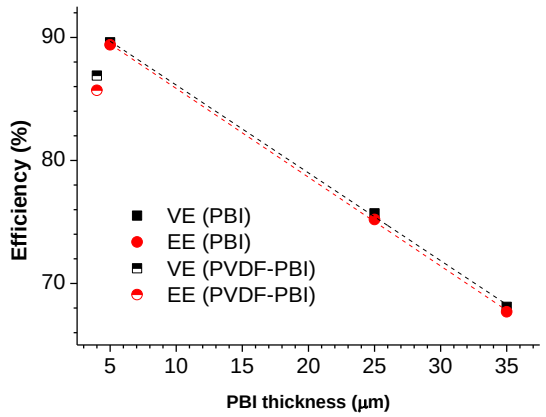

Figure 6: VE and EE of PBI membranes of different thickness (data for 25 and 35 µm thick PBI membranes is from our previous work[14])

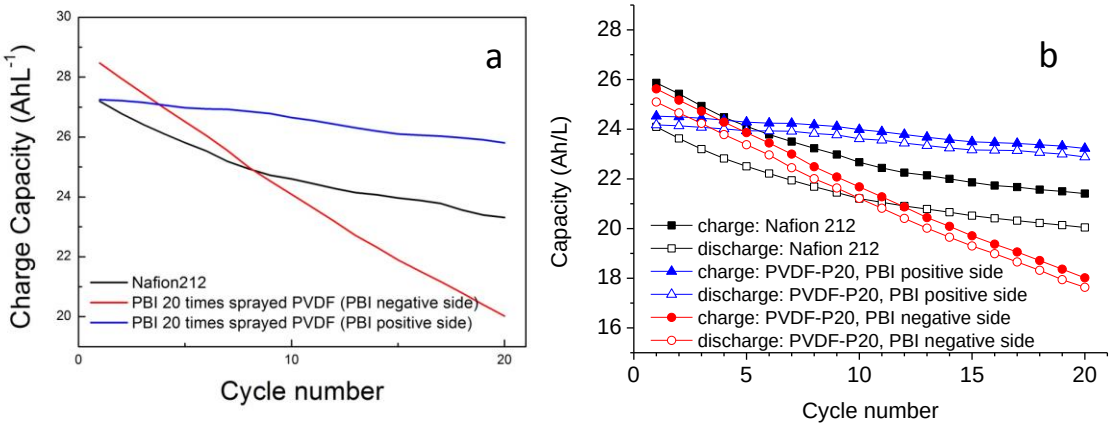

Figure 7: Changes in the charge capacity, monitored over 20-23 cycles; a) for data shown in Figure 5, b) repeat experiment**.**

As shown in **Table 1**, the reason for the strong capacity fade observed for PVDF-P20 (negative side) was a severe electrolyte imbalance. While the volume of the negative electrolyte decreased just by 2% when PVDF-P20 (positive) was used, the volume of the positive electrolyte decreased by 41% when PVDF-P20 (negative) was used. A probable but purely qualitative explanation, as schematically illustrated in **Figure 8**, is based on the following observations and assumptions:

a) Crossover of ions increases the osmotic pressure, and water will follow, to minimize osmotic pressure.

b) Crossover of vanadium ions will be mainly along the electric field, following the movement of the protons. This implies that the main contribution to crossover during charging will be from VO^{2+}/VO_2^+ ions, while crossover during the discharging step will be dominated by the crossover of V^{2+}/V^{3+} ions.

c) Concentration driven diffusion of vanadium ions through PBI membranes is low, but the application of an additional electric field may push vanadium ions over the existing energy barrier, allowing them to overcome the Donnan potential[14]. Since the voltage over the membrane is higher during charging than during discharging, we hypothesize that crossover over thin PBI membranes is higher during charging than during discharging.

Based on the above three assumptions, for PVDF-P (negative) we would expect a high VO^{2+}/VO_2^+ crossover during charging (both diffusion and migration in the electric field are high) and low V^{2+}/V^{3+} crossover during discharging (both terms, concentration driven diffusion and migration in the electric field are low), resulting in a net flow of electrolyte from the positive to the negative electrode.

In the case of PVDF-P (positive), we expect some crossover during charging: high voltage (migration in the electric field), but a low membrane potential. During discharging we expect some crossover in the opposite direction: migration in the electric field is low, but the concentration gradient is high. As a result, no large imbalance of the electrolyte is expected.

Table 1: Electrolyte balance for a cell with PVDF-P20 at the begin of test and after 20 cycles at 80 mA/cm^2.

	PBI on the positive side		PBI on the negative side	
	Begin of test	End of test	Begin of test	End of test
Negative electrolyte (V^{2+}/V^{3+})	15 ml	14.7 ml	15 ml	22 ml
Positive electrolyte (VO^{2+}/VO_2^+)	17 ml	17.3 ml	17 ml	10 ml

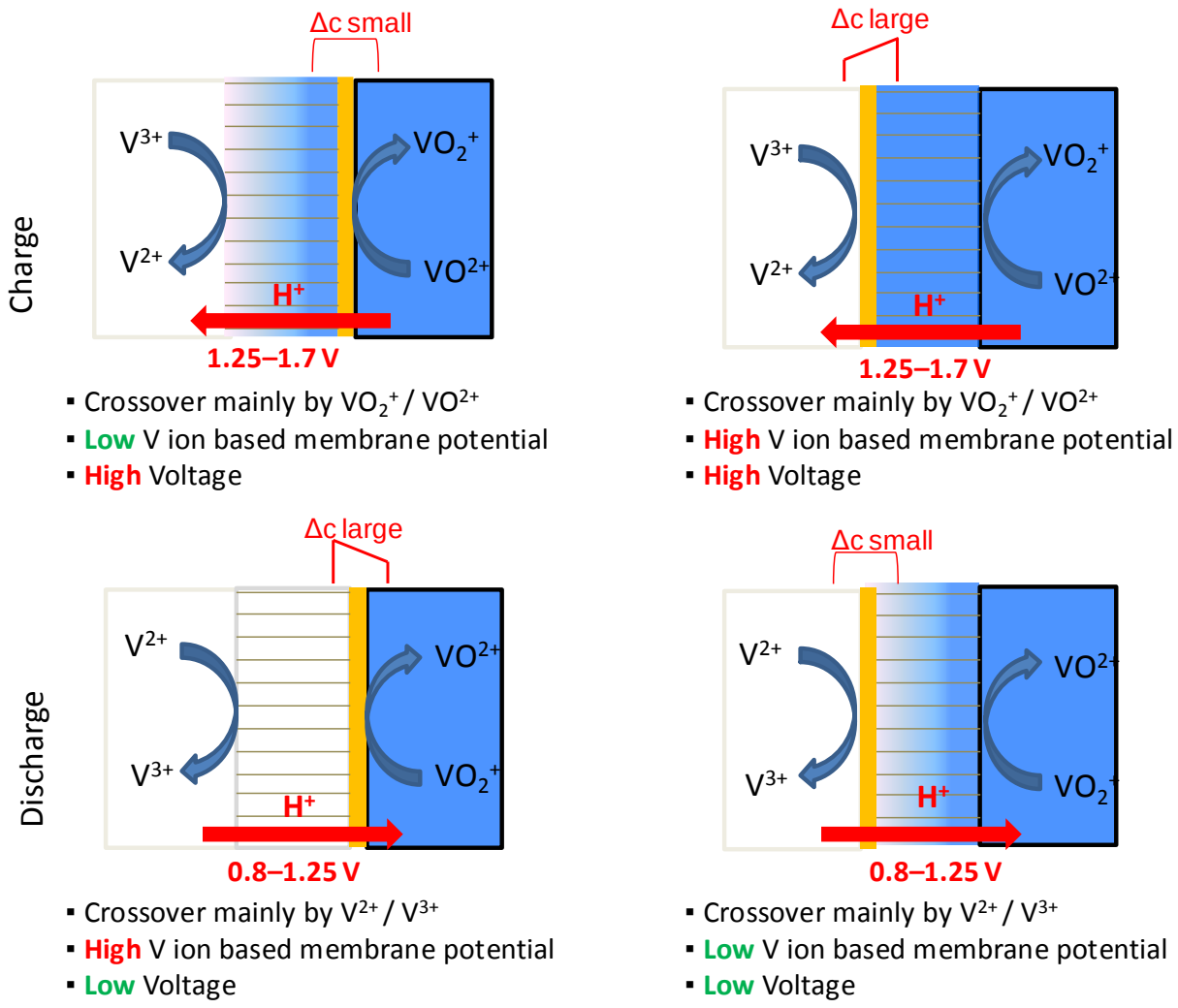

Figure 8: Considerations explaining why electrolyte imbalance and capacity fade are more pronounced when the PBI blocking layer is directed towards the negative electrolyte.

The orientation of the PBI layer towards the positive or negative electrode has also an effect on the self-discharge (**Figure 9**). While the redox-couple V^{2+}/VO_2^+ was consumed after 9.3 hours in the case of Nafion 212, cells with PVDF-P20 on the positive and negative side lasted for 10.7 and 16.4 hours, respectively. For Nafion 115, it was reported that the permeability coefficient for V^{2+} is $6.3 \cdot 10^{-7}$ cm^2 min^{-1}, 5.7, 2.5 and 4.3 times higher than for V^{3+}, VO^{2+} and VO_2^+, respectively.[39] When we assume a similar trend for Nafion 212 and PVDF-P20 membranes, we can expect that the main contribution to the self-discharge comes from V^{2+} ions moving to the positive electrolyte. When PBI is on the positive side, the concentration gradient over the membrane remains high, because V^{2+} ions diffusing to the positive electrolyte are immediately transported away by the

electrolyte passing the membrane surface. When the PBI layer faces the negative electrolyte, V^{2+} ions which crossed the membrane are inside of the PVDF pores, and the concentration gradient over the PBI later decreases, reducing the driving force for diffusion. Therefore, the self-discharge curves nicely support the hypothesis demonstrated in Figure 8, according to which the orientation of the PBI layer affects the concentration gradient over the membrane and thus the crossover.

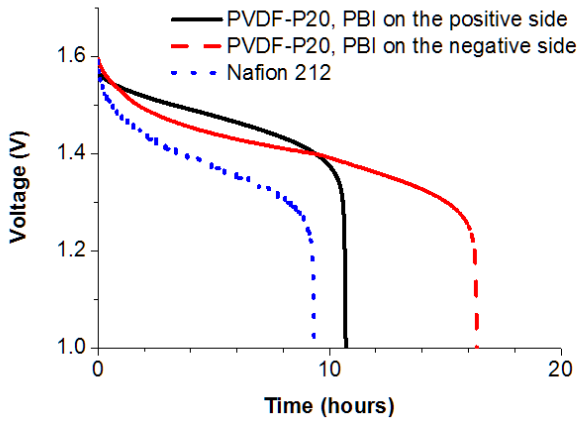

Figure 9: Self-discharge curves for cells equipped with Nafion 212 and PVDF-P20.

3.5 Upscaling

For upscaling the membrane fabrication, the process was changed from hand spraying to automated spraying. To avoid potential corrosion issues with the available machine, the spraying solution was changed from alkaline ethanol to dimethylacetamide (see supporting information for details). In this adjusted process, it was possible to spray areas of 24 cm x 28 cm. These membranes were tested in a small three-cell stack (3 x 25 cm^2). At 60 mA cm^{-2}, a stable performance over 200 cycles was observed (**Figure 10**). While the VE of the stack equipped with Nafion 117 decreased continuously, the VE and thus also the EE of the stack equipped with PVDF-P20 showed no such decrease.

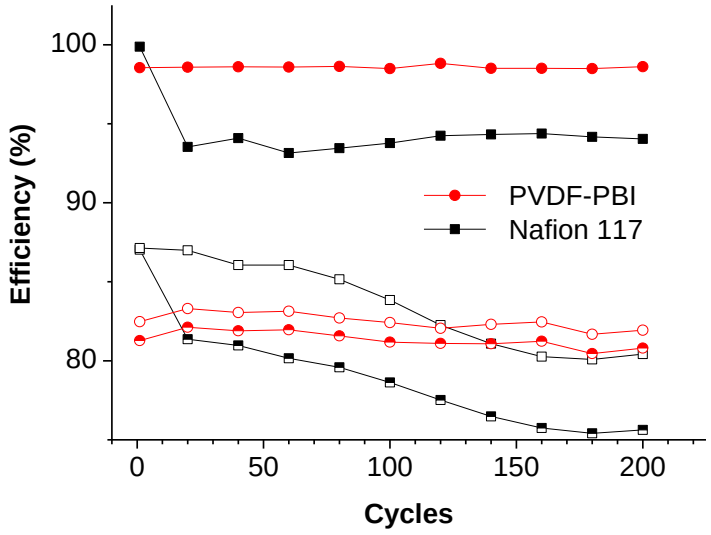

Figure 10: Coulomb (full symbols), voltage (empty symbols) and energy efficiency (half-filled symbols) for a three-cell stack, active are 25 cm^2, operated at 60 mA/cm^2. PBI faces the positive electrode.

Even though the coulomb efficiency of the stack with the PVDF-PBI membranes was significantly higher than that of Nafion 117 over all 200 cycles, the discharge capacity became similar to that of the stack with Nafion 117 after about 80 cycles (**Figure 11**). Also for the following 120 cycles the discharge capacity of the stack with Nafion 117 remained higher than that of the stack with the PVDF-PBI membrane. The exact reason for this is unknown, but we expect that the cut-off voltages were reached earlier mainly due to changes in the cell resistance, and less by cross-over.

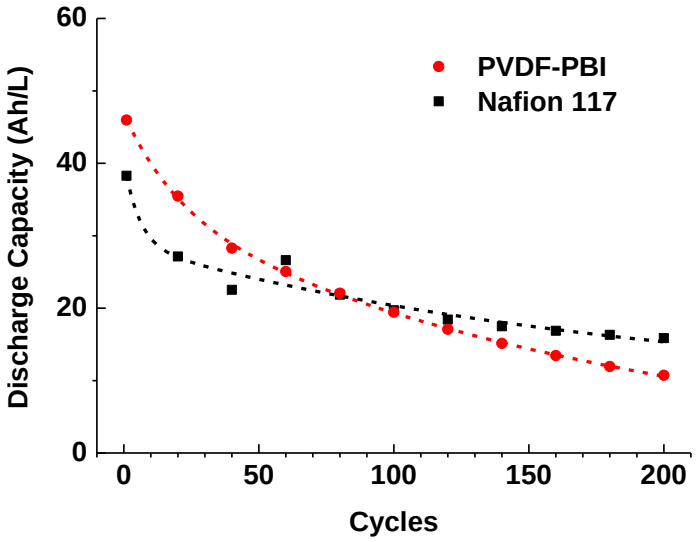

Figure 11: Discharge capacity for a three-cell stack, active are 25 cm^2, operated at 60 mA/cm^2. PBI faces the positive electrode.

4. Conclusions

A new membrane type, polybenzimidazole coated porous PVDF, was prepared by spraying a solution of PBI in ethanol/KOH on a porous PVDF membrane. As expected, adhesion between the two layers was strong, and no delamination was observed during handling, ex-situ test in 0.15 M VO_2^+ solution (**Figure S2**), and operation in the flow battery. All membranes showed lower ex-situ permeability than Nafion 211 and Nafion 212. For PVDF-P20, diffusion was so low that the measurement time needed to get reliable data needed to be extended from 4 hours to 48 hours. One striking feature was that the permeability of the coated membranes depends on the direction of the PBI layer. Permeability constants were determined to be 1.1 x 10^{-12} and 5.8 x 10^{-13} m^2 s^{-1} when the PBI layer was directed to the magnesium and the vanadium side, respectively. This behavior was explained by the formation of a low concentration gradient over the PBI layer, when the PBI layer was directed towards the vanadium rich side, and the formation of a higher membrane potential when the PBI layer was directed to the vanadium lean side, because permeated ions are immediately transported away from the PBI layer in the latter configuration.

The area specific resistance of 26.8 µm (in the wet state) thick PBI in 2M sulfuric acid was 6.6 times higher than that of Nafion 212, while that of PVDF-P20 was just 1.5 times higher. When

1.8M VO_2^+ were added to the electrolyte, the conductivity of Nafion decreased more than that of PBI.

As expected from the ex-situ data, the charge efficiency was significantly higher for PVDF-P20 membranes than for Nafion 212. The highest CE was observed when the membrane was oriented to the positive electrolyte. Because of a rather similar voltage efficiency, the energy efficiency of PVDF-P20 membranes was higher than that of Nafion 212.

An important finding was the strong effect which the orientation of the PBI blocking layer has on the charge capacity during cycling. Reproducibly, cells showed the lowest capacity fade when the PBI layer was directed towards the positive electrolyte, and the highest capacity fade when the PBI layer was directed to the negative electrolyte. A qualitative explanation for this behavior is given.

In summary, coating of porous support structures with a 4 µm thin PBI blocking layer provided access to membranes which showed better VRFB performance than Nafion 212 in the VRFB in terms of CE, EE and capacity fade during cycling. Future research will be aimed at optimising the porous support in regard to material, porosity and thickness. We expect that smaller pores will lead to stronger PBI layers with a reduced number of defects.

Conflicts of interest

There are no conflicting interests.

Acknowledgements

This work was supported by the German-Korean joint SME R&D projects program of MOTIE/KIAT (No. 20151732) and by the Korea Institute of Energy Technology Evaluation and Planning (KETEP) and the Ministry of Trade, Industry & Energy (MOTIE) of the Republic of Korea (No. 20172420108550) and by the National Research Foundation of Korea (NRF) and the Ministry of Education (MOE) (No. 2019R1A2C1005776).

References

[1] W. Kangro, H. Pieper, Zur Frage der Speicherung von Elektrischer Energie in Flüssigkeiten, Electrochim. Acta 17 (1962) 435-448. https://doi.org/10.1016/0013-4686(62)80032-2

[2] W. Kangro, Verfahren zur Speicherung von elektrischer Energie, German Patent, DE914264, 1949.

[3] W. Lee, B.W. Kwon, Y. Kwon, Effect of carboxylic acid doped carbon nanotube catalyst on the performance of aqueous organic redox flow battery using the modified alloxazine and ferrocyanide redox couple, ACS Appl. Mater. Interfaces, 10 (2018) 36882-36891. https://doi.org/10.1021/acsami.8b10952

[4] W. Lee, A. Permatasari, B.W. Kwon, Y. Kwon, Performance evaluation of aqueous organic redox flow battery using anthraquinone-2,7-disulfonic acid disodium salt and potassium iodide redox couple, Chem. Eng. J. 358 (2019) 358, 1438-1445. https://doi.org/10.1016/j.cej.2018.10.159

[5] M. Skyllas-Kazacos, M. Rychcik, R. G. Robins, A. G. Fane, M. A. Green, New All-Vanadium Redox Flow Cell, J. Electrochem. Soc. 133 (1986) 1057-1058. https://doi.org/10.1149/1.2108706

[6] C. Noh, B.W. Kwon, Y. Chung, Y. Kwon, Effect of the redox reactivity of vanadium ions enhanced by phosphorylethanolamine based catalyst on the performance of vanadium redox flow battery, J. Power Sources 406 (2018) 26-34. https://doi.org/10.1016/j.jpowsour.2018.10.042

[7] C. Noh, C. Lee, W.S. Chi, Y. Chung, J. Kim, Y. Kwon, Vanadium Redox Flow Battery Using Electrocatalyst Decorated with Nitrogen-Doped Carbon Nanotubes Derived from Metal-Organic Frameworks, J. Electrochem. Soc. 165 (2018) A1388-A1399. https://doi.org/10.1149/2.0621807jes

[8] https://www.elektormagazine.com/news/storing-wind-power-in-a-giant-flow-battery, accessed 2018.03.30

[9] W. Wang, Q. Luo , B. Li , X. Wei, L. Li, Z. Yang, Recent Progress in Redox Flow Battery Research and Development, Adv. Funct. Mater. 23 (2013) 970–986. https://doi.org/10.1002/adfm.201200694

[10] R. Ye, D. Henkensmeier, S. J. Yoon, Z. Huang, D. K. Kim, Z. Chang, S. Kim, R. Chen, Redox Flow Batteries for Energy Storage: A Technology Review, J. Electrochem. En. Conv. Stor. 15 (2018) 010801. https://doi.org/10.1115/1.4037248

[11] Z. Yuan, X. Li, Y. Zhao, H. Zhang, Mechanism of Polysulfone-Based Anion Exchange Membranes Degradation in Vanadium Flow Battery, ACS Appl. Mater. Interfaces 7 (2015) 19446-19454. https://doi.org/10.1021/acsami.5b05840

[12] X.L. Zhou, T.S. Zhao, L. An, L. Wei, C. Zhang, The use of polybenzimidazole membranes in vanadium redox flow batteries leading to increased coulombic efficiency and cycling performance, Electrochim. Acta. 153 (2015), 492-498. https://doi.org/10.1016/j.electacta.2014.11.185

[13] J.-K. Jang, T.-H. Kim, S. J. Yoon, J. Y. Lee, J.-C. Lee, Y. T. Hong, Highly proton conductive, dense polybenzimidazole membranes with low permeability to vanadium and enhanced H_2SO_4 absorption capability for use in vanadium redox flow batteries, J. Mater. Chem. A, 2016, 4, 14342-14355. https://doi.org/10.1039/c6ta05080h

[14] C. Noh, M. Jung, D. Henkensmeier, S.-W. Nam, Y. Kwon, Vanadium Redox Flow Batteries Using meta-Polybenzimidazole-Based Membranes of Different Thicknesses, ACS Applied Mater. Interfaces 9 (2017) 36799-36809. https://doi.org/10.1021/acsami.7b10598

[15] Z. Yuan, Y. Duan, H. Zhang, X. Li, H. Zhang, I. Vankelecom, Advanced porous membranes with ultra-high selectivity and stability for vanadium flow batteries, Energy Environ. Sci. 9 (2016) 441-447. https://doi.org/10.1039/c5ee02896e

[16] S. Peng, X. Yan, X. Wu, D. Zhang, Y. Luo, L. Su, G. He, Thin skinned asymmetric polybenzimidazole membranes with readily tunable morphologies for high-performance vanadium flow batteries, RSC Adv. 7 (2017) 1852-1862. https://doi.org/10.1039/C6RA24801B

[17] S. Maurya, S.-H. Shin, J.-Y. Lee, Y. Kim, S.-H. Moon, Amphoteric nanoporous polybenzimidazole membrane with extremely low crossover for a vanadium redox flow battery, RSC Adv. 6 (2016) 5198–5204. https://doi.org/10.1039/C5RA26244E

[18] X. L. Zhou, T. S. Zhao, L. An, Y. K. Zeng, X. B. Zhu, Performance of a vanadium redox flow battery with a VANADion membrane, Appl. Energy 180 (2016) 353–359. https://doi.org/10.1016/j.apenergy.2016.08.001

[19] I. S. Chae, T. Luo, G. H. Moon, W. Ogieglo, Y. S. Kang, M. Wessling, Ultra-High Proton/Vanadium Selectivity for Hydrophobic Polymer Membranes with Intrinsic Nanopores for Redox Flow Battery, Adv. Energy Mater.6 (2016) 1600517. https://doi.org/10.1002/aenm.201600517

[20] J. Ma, S. Wang, J. Peng, J. Yuan, C. Yu, J. Li, X. Ju, M. Zhai, Covalently incorporating a cationic charged layer onto Nafion membrane by radiation-induced graft copolymerization to reduce vanadium ion crossover, Europ. Polym. J. 49 (2013) 1832–1840. https://doi.org/10.1016/j.eurpolymj.2013.04.010

[21] J. grosse Austing, C. Nunes Kirchner, L. Komsiyska, G. Wittstock, Layer-by-layer modification of Nafion membranes for increased life-time and efficiency of vanadium/air redox flow batteries, J. Membr. Sci. 510 (2016) 259–269. https://doi.org/10.1016/j.memsci.2016.03.005

[22] F. J. Oldenburg, E. Nilsson, T. J. Schmidt, L. Gubler, Tackling Capacity Fading in Vanadium Redox Flow Batteries with Amphoteric PBI/Nafion Bilayer Membranes, ChemSusChem, 2019, https://doi.org/10.1002/cssc.201900546

[23] S. Kim, S. Yuk, H. G. Kim, C. Choi, R. Kim, J. Y. Lee, Y. T. Hong, H.-T. Kim, A hydrocarbon/Nafion bilayer membrane with a mechanical nano-fastener for vanadium redox flow batteries, J. Mater. Chem. A 5 (2017) 17279–17286. https://doi.org/10.1039/C7TA02921G

[24] S. M. Ahn, H. Y. Jeong, J.-K. Jang, J. Y. Lee, S. So, Y. J. Kim, Y. T. Hong, T.-H. Kim, Polybenzimidazole/Nafion hybrid membrane with improved chemical stability for vanadium redox flow battery application, RSC Adv. 8 (2018) 25304–25312. https://doi.org/10.1039/C8RA03921F

[25] M. Jung, W. Lee, N. Nambi Krishnan, S. Kim, G. Gupta, L. Komsiyska, C. Harms, Y. Kwon, D. Henkensmeier, Porous-Nafion/PBI composite membranes and Nafion/PBI blend membranes for Vanadium Redox Flow Batteries, Appl. Surface Sci. 450 (2018) 301–311. https://doi.org/10.1016/j.apsusc.2018.04.198

[26] L. Gubler, F.J. Oldenburg, A. Schneider, T.J. Schmidt , D. Vonlanthen, Amphoteric and Bilayer Membranes for Vanadium Redox Flow Batteries, ACS Workshop: Polymers for Fuel Cells, Energy Storage, and Conversion, Asilomar Conference Grounds, Pacific Grove (CA), USA, Feb 24 – 27, 2019.

[27] H. Ahmad, S. K. Kamarudin, U. A. Hasran,W. R. W. Daud, Overview of hybrid membranes for direct-methanol fuel-cell applications, Int. J. Hydrogen Energy 35 (2010) 2160-2175. https://doi.org/10.1016/j.ijhydene.2009.12.054

[28] L. Zhang, Q.-Q. Ni, A. Shiga, Y. Fu, T. Natsuki, Synthesis and Mechanical Properties of Polybenzimidazole Nanocomposites Reinforced by Vapor Grown Carbon Nanofibers, Polym. Composites 31 (2010) 491-496. https://doi.org/10.1002/pc.20829

[29] L. Semiz, N. D. Sankir, M. Sankir, Directly Copolymerized Disulfonated Poly(arylene ether sulfone) Membranes for Vanadium Redox Flow Batteries, Int. J. Electrochem. Sci. 9 (2014) 3060 - 3067.

[30] D. Chen, M. A. Hickner, E. Agar, E. C. Kumbur, Optimized Anion Exchange Membranes for Vanadium Redox Flow Batteries, ACS Appl. Mater. Interfaces 5 (2013) 7559–7566. https://doi.org/10.1021/am401858r

[31] B. Jiang, L. Yu, L. Wu, D. Mu, L. Liu, J. Xi, X. Qiu, Insights into the Impact of the Nafion Membrane Pretreatment Process on Vanadium Flow Battery Performance, ACS Appl. Mater. Interfaces 8 (2016) 12228−12238. https://doi.org/10.1021/acsami.6b03529

[32] B. Jiang, L. Wu, L.Yu, X. Qiu, J. Xi, A comparative study of Nafion series membranes for vanadium redox flow batteries, J. Membr. Sci. 510 (2016) 18–26. https://doi.org/10.1016/j.memsci.2016.03.007

[33] Z. Tang, R. Svoboda, J. S. Lawton, D. S. Aaron, A. B. Papandrew, T. A. Zawodzinski, Composition and Conductivity of Membranes Equilibrated with Solutions of Sulfuric Acid and Vanadyl Sulfate, J. Electrochem. Soc. 160 (2013) F1040-F1047. https://doi.org/10.1149/2.083309jes

[34] Y. Lee, S. Kim, R. Hempelmann, J. H. Jang, H.-J. Kim, J. Han, J. Kim, D. Henkensmeier, Nafion membranes with a sulfonated organic additive for the use in vanadium redox flow batteries, J. Appl. Polym. Sci. 136 (2019), 47547. https://doi.org/10.1002/app.20182977.

[35] M. Jung, W. Lee, C. Noh, A. Konovalova, G. S. Yi, S. Kim, Y. Kwon, D. Henkensmeier, Blending polybenzimidazole with an anion exchange polymer increases the efficiency of Vanadium Redox Flow Batteries, J. Membr. Sci. 2019, 580, 110-116. https://doi.org/10.1016/j.memsci.2019.03.014

[36] S. Kumar, S. Jayanti, High Energy Efficiency With Low-Pressure Drop Configuration for an All-Vanadium Redox Flow Battery, J. Electrochem. En. Conv. Stor. 13 (2017) 041005. https://doi.org/10.1115/1.4035847

[37] T. Luo, O. David, Y. Gendel, M. Wessling, Porous poly(benzimidazole) membrane for all vanadium redox flow battery, J. Power Sources 312 (2016) 45-54. https://doi.org/10.1016/j.jpowsour.2016.02.042

[38] B. Shanahan, T. Böhm, B. Britton, S. Holdcroft, R. Zengerle, S. Vierrath, S. Thiele, M. Breitwieser, 30 μm thin hexamethyl-*p*-terphenyl poly(benzimidazolium) anion exchange membrane for vanadium redox flow batteries, Electrochem. Commun. 102 (2019) 37-40. https://doi.org/10.1016/j.elecom.2019.03.016

[39] J. Sun, D. Shi, H. Zhong, X. Li, H. Zhang, Investigations on the self-discharge process in vanadium flow battery, J. Power Sources 294 (2015) 562-568. https://dx.doi.org/10.1016/j.jpowsour.2015.06.123